

## Investigation about maximum rise of trajectory of 30° and 45° inclined dense jets

Fariborz Mohammadi<sup>1</sup>; Heydar Ali Kashkuli<sup>1</sup>; Saied Boroomand nasab<sup>1</sup>; Abd Ali Naseri<sup>1</sup>; Javad Ahadian<sup>1</sup>

1- Department of Irrigation and Drainage, Water Science faculty, Chamran university of Ahwaz, Ahwaz, Iran.  
[Mo.fariborz@gmail.com](mailto:Mo.fariborz@gmail.com)

**Abstract:** This paper reports experimental and mathematical results of an investigation of inclined round buoyant jets in a stationary ambient. The experiments were conducted in a glass-walled channel 7 m long by 0.72 m wide by 0.7 m deep. The visual dimensionless maximum height of trajectory rise and the relatively horizontal location as a function of densimetric Froude number is investigated at brine jet angles 45° and 60° towards the horizon. The various results of previous studies has caused confusion arise in this field. Using different methods to capturing the trajectory properties and choose different range of Froude number in various studies are two main reasons for this problem. The range of Froude number in this study was 5.3 to 15.6. The dimensionless  $Z_{\max}/D$  number changes as a function of Froude number is fairly linear. Slope of The trend line is the same at both jet angle 45° and 60°. This suggests that changes in Froude value have the same effect on the dimensionless  $Z_{\max}/FrD$  number at both jet angles. The results of mathematical model are shown that the Flow-3D has a good Capability to simulate the maximum rise and the horizontal distance of it.

[Mohammadi F, Kashkuli HA, Boroomand nasab S, Naseri AA, Ahadian J. **Investigation about maximum rise of trajectory of 30° and 45° inclined dense jets.** *Nat Sci* 2012;10(11):188-194]. (ISSN: 1545-0740). <http://www.sciencepub.net/nature>. 28

**Key words:** round buoyant jet, terminal of trajectory, brine disposal, stagnant ambient

### 1. Introduction:

In recent decades world's population is growing very fast, particularly in the Middle East. To provide the food needed for the world's population, cultivation agricultural land area has grown at a rapid pace. Consequently, volume of brine drainage production is also increased. The saline effluents are usually discharged into rivers and lakes and are denser than the ambient. Also, to provide fresh water resource supplies to deal with water scarcity, desalination plants of seawater established (e.g. Jubail, Saudi Arabia at Persian Gulf). Produce fresh water from sea water lead to concentrated brine which must be disposed properly to sea. The traditional and the simplest form of disposing of the buoyant discharge is a surface discharge or a fall by a pipe at the shoreline. The form of disposal is not suitable because of its low mixing and high concentration of pollutants at shoreline zone. Consequently, in the most industrialized countries, quality and mixing zone regulation of Water, banned or dispirited the surface discharge mode. To reach most initial dilution, usually disposal of buoyant discharges are by negative buoyant jets.

Environmental and ecological concerns make the initial dilution of disposal the brine waste water into ambient as an important subject (e.g. includes the brine discharge of large-scale desalination plants In Persian Gulf). A review of researches on the extent and intensity of brine plumes in receiving waters surrounding desalination plant discharge showed that in some cases it is

approximately 4000 meters from the outlet (Roberts, 2010), (Sadhvani, 2005) Usually the reaction of fauna and flora of ambient to brine disposal is related to the concept of "mixing zone". Mixing zone is an area that ambient quality parameters have been affected by brine disposal (Jirka, 2004). The environmental impact of brine discharge to sea is investigated in some several research and its adverse impacts on marine fauna and flora is mentioned (Fernandez-Torquemeda et al., 2005, Gacia et al., 2007 and Iso et al., 1994).

Jet angle to the horizon is one of the most important parameters in determining the initial dilution of negative buoyant jets. So far, many studies have been done about it. One of the first systematic studies in this field has been conducted by Zeitoun et al (1970). Their experiments were at the rate of initial dilution jets oblique angles of 30, 45, 60 and 90 ° relatively to the horizon and carried out in stagnant ambient. Their results showed that initial dilution in jet oblique angle 60 degrees is more than the other angles. The results of the study have been approved by research of Pincince and List (1973), Roberts and Tom (1987) and Roberts et al (1997) as in stagnant ambient and cross flow.

However, the results of Corjet showed that initial dilution of jets at maximum height of rise in an angle of 45 degrees is a bit more of an angle of 30 and 60 (Jirka, 2004 and Jirka, 2008).

It is noteworthy that before him, Cederwall (1968) has shown that brine disposal at 45-degree

angle to achieve maximum dilution, is more suitable than other angles.

To date, several Integral and numerical models have been developed for determining the trajectory parameters of submerged negative buoyant jets. But according to the complexity of this phenomenon, so far the models were not able to simulate accurately the characteristics of dilution of negative buoyant jets (Jirka 2004, 2008, Bleninger, 1997, Doneker, 2006 and Lai and Lee, 2012).

Furthermore what about the angle effect on the jet in the initial dilution mentioned, the jet angle is very important in the shallow ambient. The possibility of jet impingement on surface water will increase by increasing jet angle to the horizon. As a result of jet impingement on water surface will decrease the amount of initial dilution (Doneker et al., 1991). Hence, the peak of trajectory in design of the jet in shallow waters has major importance. So far, many investigations have been performed on the peak of trajectory. Some examples are including the investigations of Anwar, 1969, Zeitoun et al., 1970, Roberts et al., 1997, Bloomfield, 2002 and Cipollina et al., 2005. One of the main reasons for continuing research in this area is the invention of new computing devices and measurement. So that the progress of measuring devices, allow for more accurate measurements of parameters of submerged jets is provided. But the main reason for continuing these studies is the mismatch of the results of different investigators (Lai and Lee, 2012). Moreover, so far none of commercial models have succeeded to simulate parameters of dense jets completely (Palomar et al., 2012).

This research reports series of experimental investigation of maximum rise of trajectory in angles 45 and 60 degrees of negative brine jets in stationary ambient. Also a three-dimensional model was used to study numerically the experiments, along with its maximum rise, of brine water discharged from submerged jets in shallow water.

At first the theoretical framework for dimensional analysis is presented. Then, the experimental design and procedure of experiments are presented. Subsequently, the data obtained from the experiments and numerical models are presented. Finally, Analysis of experimental and numerical model's results will be discussed.

## 2. Materials and Methods

### 2.1. Dimensional analysis

Figure 1 shows a schematic view of disposal negative submerged dense jet in stationary ambient. The jet is discharged at angle  $\Theta_0$  degrees to the horizon with jet diameter  $D$ , jet velocity at entrance  $V_j$  and the initial jet density  $\rho_j$  that is larger than

ambient density  $\rho_a$ . The jet moves upward to reach to peak of its trajectory then at this point, As a result of buoyancy force continues its move in the trajectory downward path. The maximum rise of jet  $Z_t$ , depends on the initial density difference  $\Delta\rho = \rho_j - \rho_a$ ,  $V_j$ ,  $D$  and  $\Theta_0$ . The ratio between inertia and viscous forces is determined by the Reynolds number. In all experiments its value was sufficiently high, as will always be the practical case, the flow was fully turbulent and viscous forces was neglected. Also, the brine jet trajectory depends mainly on the ratio of inertial to buoyancy forces, which is expressed by the densimetric Froude number. It can be defined

as  $Fr = \frac{U_j}{\sqrt{g'D}}$ , where  $g$ =gravitational acceleration

and  $g' = \frac{\rho_j - \rho_a}{\rho_a} g$  is the initial value of the adjusted

acceleration due to gravity. In the present study, the jet trajectory characteristics of interest are the prediction of maximum rise height  $Z_t$  and The horizontal distance from the jet exit to the peak of trajectory  $X_t$ .

By dimensional analysis, it can be tangible that  $Z_t$  and  $X_t$  for the brine jet trajectory can be stated in terms of the discharge conditions as:

$$\frac{X_t}{FrD} = f(Fr, \theta) \tag{1}$$

$$\frac{Z_t}{FrD} = f(Fr, \theta) \tag{2}$$

The functional dependence  $f(Fr, \theta)$  must be determined from experimental data.

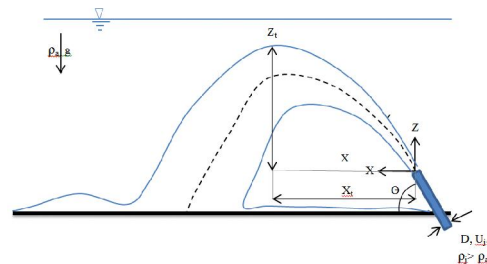


Figure 1. An inclined submerged negative buoyant round jet in stagnant ambient

### 2.2. Numerical modeling

In the present study, the CFD package FLOW-3D has been used for numerical modeling. The commercially available CFD package FLOW-3D uses a Cartesian coordinate system to modeling the turbulent flow of incompressible fluid with buoyancy (Flow Science, 2003). The governing equations in this system follow time-averaging fully three-dimensional continuity, momentum, energy transport, and the equation of state. The FLOW-3D uses the finite

difference method to solve the above RANS equations (Kim n.d.). According to the result of studies of Kim and Cho (2006), Yakhot and Orszag (1986) and Yakhot et al. (1992) a two equation  $Re$  Normalized Group (RNG) turbulence model was used for turbulence closure. In the computational domain is used an orthogonal mesh definition in terms of Cartesian coordinates. For each cell, mean values for the flow parameters are calculated at discrete times using a staggered grid method. A complete Description of the numerical model used in this study is presented by Kim and Cho (2006).

## 2.3. Experimental setup and procedure

### 2.3.1. Apparatus

The experiments were conducted in a glass-walled channel 7 m long by 0.72 m wide by 0.7 m deep. A Plexiglas floor was placed in the channel through which the Plexiglas nozzle has entered From floor the channel and its diameter was 0.011m. Despite the cutting-edge nozzle by laser, very small rough surfaces at the edge nozzle of laser have been observed. The rough surfaces were deformed the circular shape of the jet. To resolve this problem a turning aluminum nozzle with the same outer diameter at end of Plexiglas nozzle was used. The height of nozzle tip above the floor channel was 50 mm, allowing adequate room to avoid the bottom boundary effect. Brine was a mixture of water and salt. To record more accurate observation data, brine was dyed. For this purpose, 10 gr/m<sup>3</sup> of potassium permanganate is used. The amount of dye did not make changes in the jet density. The exact density of

the jet fluid and the ambient fluid was measured by a Mettler Toledo density meter (model Density 30Px). Brine is made in a tank 1m long by 1m wide by 1m deep. The jet discharge is fed from the tank by a pump. In order to inject different discharge to channel a valve is used in transition pipe from brine tank to channel. The distance of valve to jet exit is more than 100D. A Magab electromagnetic flow meter (model 3000) is used to measure the jet discharge. Before each experiment, the channel is filled with tap water to a height of 50 cm and it was fixed for all experiments. After each experiment channel is rinsed by tap water and is filled with tap water again for next experiment. Observation data is recorded by Sony Cyber-shot camera (model DSC-RX100/B) and channel wall is scaled by transparent rulers. Since each experiment began, the images of brine jet were captured for 60 seconds. Then,  $Z_t$  and  $X_t$  data were extracted from images. The experimental configuration is sketched in Figure 2.

### 2.3.2. Procedure

Before each experiment, the Jet fluid by mixing the tap water and salt in the brine tank is provided with a certain density. The channel has been filled with tap water to a height of 50 cm. The density and temperature of the ambient and brine is determined using a density meter. Brine is injected into the channel with the desired discharge using jet valve. The jet discharge is recorded by the flow meter.  $Z_t$  and  $X_t$  data is captured by camera. A summary of the experimental parameters is given in Table 1.

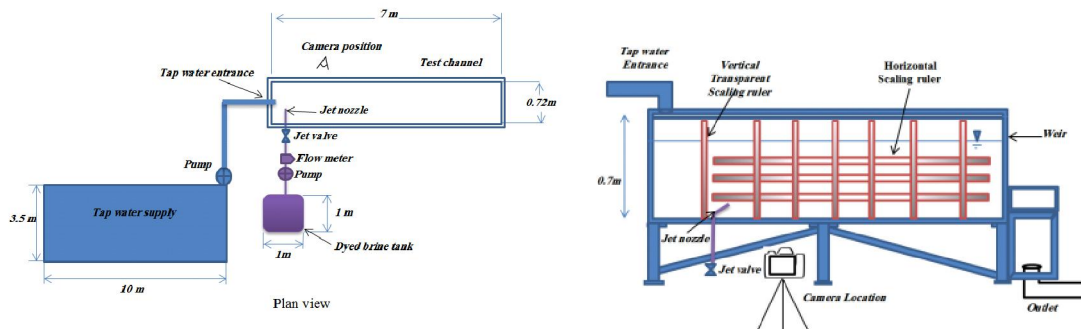


Figure 2. Schematic Depiction of Experimental Configuration

Table 1. Experimental parameters of inclined round dense jet in stationary ambient (jet diameter D = 11.1 mm)

| Jet discharge flow<br>Qo (m3/hr) | Ambient density<br>pa (g/cm3) | Jet density<br>pj (g/cm3) | Ambient temperature<br>Ta (°C) | Jet temperature<br>Tj (°C) | Jet densimetric<br>Froud number Fr | Jet Reynolds<br>number Re |
|----------------------------------|-------------------------------|---------------------------|--------------------------------|----------------------------|------------------------------------|---------------------------|
| Jet angle, $\Theta=45$           |                               |                           |                                |                            |                                    |                           |
| 0.147                            | 0.9936                        | 1.0152                    | 31                             | 33.2                       | 8.9                                | 4729                      |
| 0.197                            | 0.9939                        | 1.0128                    | 31.5                           | 32.97                      | 12.7                               | 6337                      |
| 0.23                             | 0.9928                        | 1.0166                    | 32.5                           | 34.2                       | 13.2                               | 7399                      |
| 0.234                            | 0.9938                        | 1.0123                    | 29.7                           | 32.9                       | 15.3                               | 7528                      |
| 0.265                            | 0.9925                        | 1.0257                    | 34                             | 34.9                       | 12.9                               | 8525                      |
| 0.296                            | 0.9926                        | 1.0257                    | 33                             | 32.2                       | 14.4                               | 9522                      |
| 0.239                            | 0.9924                        | 1.0144                    | 33.1                           | 33.7                       | 14.3                               | 7688                      |
| 0.241                            | 0.9923                        | 1.0152                    | 33.3                           | 33.3                       | 14.1                               | 7753                      |
| 0.147                            | 0.9926                        | 1.0173                    | 33.2                           | 34.2                       | 8.3                                | 4729                      |
| 0.165                            | 0.9932                        | 1.0161                    | 31.6                           | 32                         | 9.7                                | 5308                      |
| 0.241                            | 0.9937                        | 1.0174                    | 31.2                           | 31.9                       | 13.9                               | 7753                      |
| 0.232                            | 0.9943                        | 1.0206                    | 30.6                           | 31.3                       | 12.7                               | 7463                      |
| 0.311                            | 0.9932                        | 1.0902                    | 31.6                           | 32.7                       | 8.9                                | 10005                     |
| 0.395                            | 0.9931                        | 1.0915                    | 32                             | 31.4                       | 11.2                               | 12707                     |
| 0.437                            | 0.9921                        | 1.0935                    | 31                             | 32                         | 12.2                               | 14058                     |
| 0.238                            | 0.9921                        | 1.0334                    | 34.2                           | 34.4                       | 10.4                               | 7656                      |
| 0.247                            | 0.9924                        | 1.035                     | 33.2                           | 35.1                       | 10.6                               | 7946                      |
| 0.362                            | 0.9935                        | 1.0358                    | 31.9                           | 32.8                       | 15.6                               | 11645                     |
| Jet angle, $\Theta=60$           |                               |                           |                                |                            |                                    |                           |
| 0.296                            | 0.9928                        | 1.0669                    | 31.6                           | 33.6                       | 9.6                                | 9522                      |
| 0.41                             | 0.9951                        | 1.0666                    | 33.7                           | 34.4                       | 13.6                               | 13189                     |
| 0.142                            | 0.9931                        | 1.0222                    | 33.6                           | 34.7                       | 7.4                                | 4568                      |
| 0.189                            | 0.9933                        | 1.0223                    | 32                             | 32.6                       | 9.8                                | 6080                      |
| 0.191                            | 0.9951                        | 1.0967                    | 33.1                           | 33.4                       | 5.3                                | 6144                      |
| 0.22                             | 0.998                         | 1.0651                    | 32                             | 33.2                       | 7.6                                | 7077                      |
| 0.228                            | 0.9945                        | 1.1002                    | 32.7                           | 33.9                       | 6.2                                | 7334                      |
| 0.259                            | 0.996                         | 1.0218                    | 34.6                           | 34.4                       | 14.3                               | 8332                      |
| 0.385                            | 0.9937                        | 1.0969                    | 33.7                           | 34.6                       | 10.6                               | 12385                     |

**3. Result**

**3.1. Experimental results**

In these experiments, time required to form a stable trajectory was about 15 to 20 seconds. A typical instantaneous image of experiments (the last experiment jet angle  $\Theta=45$ ) is shown in Figure 3.

**3.1.1. The maximum height of rise**

Figure 4 shows the visual dimensionless maximum height of rise as a function of the initial Froude number. As shown in Figure 4, the dimensionless  $Z_{max}/D$  number changes as a function of Froude number is fairly linear. Slope of The trend line is the same at both jet angle  $45^\circ$  and  $60^\circ$ . This suggests that changes in Froude value have the same effect on the dimensionless  $Z_{max}/D$  number at both jet angles. It is worth noting that in this study, the Froude number changes was due to the jet velocity and the density difference between the ambient and the jet fluid. Therefore, in this study the effect of nozzle diameter on the Froude number and subsequently the changes in the dimensionless  $Z_{max}/D$  number is not investigated.

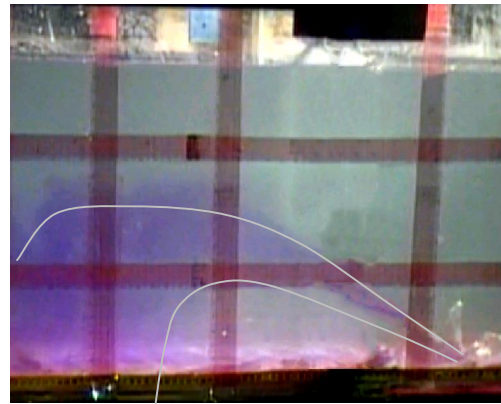


Figure 3. Typical instantaneous image of Dense Jet:

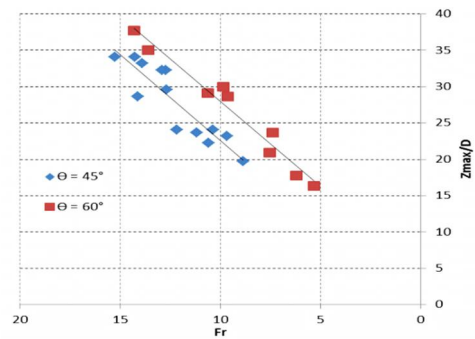


Figure 4. Measured visual Zmax against Fr

Figure 5 shows the visual dimensionless maximum height of rise  $Z_{max}/FrD$  as a function of the jet discharge Froude number  $Fr$  for jet discharge angles  $45^\circ$  and  $60^\circ$  in stationary ambient. As is shown in Figure 5, at an angle of  $60^\circ$ , Dimensionless number  $Z_{max}/FrD$  is in the range of 2.57 to 3.2 and at jet inclined  $45^\circ$  is in the range of 2 to 2.8. The average value of  $Z_{max}/FrD$  for jet angle  $45^\circ$  and  $60^\circ$  is 2.28 and 2.87, respectively. In comparison with previous research, the average values of  $Z_{max}/FrD$  in this study are higher than other studies. as mentioned before, the range of Froude number in this study was 5.3 to 15.6. The ranged Froude number is the smallest ranged studies conducted so far. The main reason for this issue is the range of Froude number of experiments has been performed. Some of the results of previous experimental and mathematical modeling and the current study are listed in table 2.

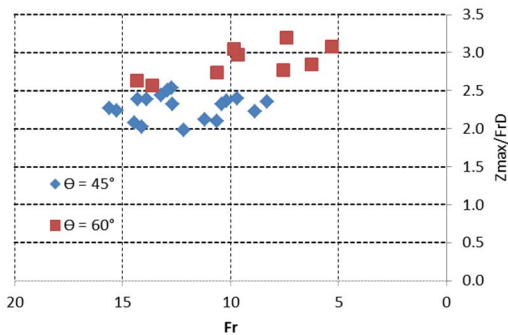


Figure 5. The experiments results of maximum rise height

### 3.1.2. The horizontal location at $Z_{max}$

As mentioned earlier, the horizontal location at  $Z_{max}$  is one of the most effective parameters on dilution of the dense jet. Figure 6 shows the dimensionless horizontal location at maximum rise to the Froude densimetric number.

At a certain angle, the initial dilution increases by increasing  $X_t$ . This part of the trajectory is affected by momentum. In this region, the shear layer surrounding the trajectory is affected by jet momentum. Then, the vortex formation Due to

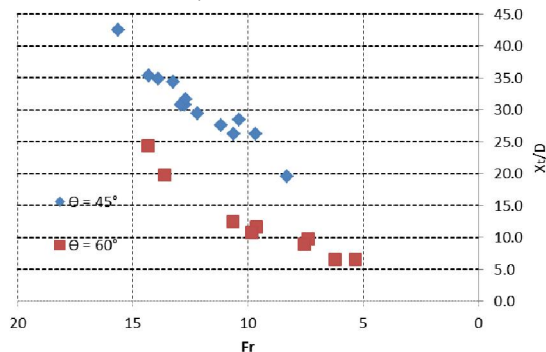


Figure 6. Measured visual  $X_t$  against  $Fr$

shear layer around trajectory will be drawn at large volume of ambient fluid into the jet. Accordingly, the horizontal location at  $Z_{max}$  is one of the most important parameters in the design of the brine jet to effluent disposal.

Figure 7 shows the visual the horizontal distance from  $Z_{max}$  to jet entrance, and  $X_t/FrD$ , as a function of the jet discharge Froude number  $Fr$  for jet discharge angles  $45^\circ$  and  $60^\circ$  in stationary ambient.

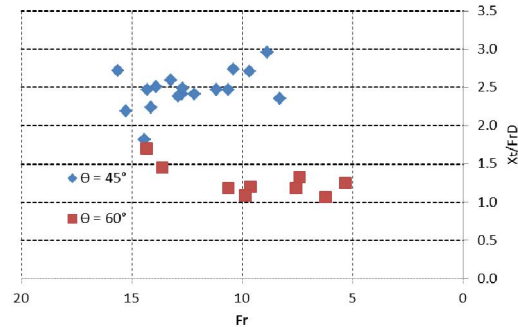


Figure 7. The experiments results of the horizontal distance from  $Z_{max}$  to jet entrance

According to the results shown in Table 2, it can be seen that experimental results on the parameter  $X_t/FrD$  in the present study is close to the Papakonstantis et al. 2011, results. As shown in Table 2, among the studies conducted about determining  $X_t$ , the results of Lai and Lee 2012, is very different from other research. Perhaps one of the reasons for the results difference is using various methods of recording date. Another reason that can be cited in this regard has conducted research in different periods Froude number. The comparison Lai and Lee 2012, with Shao Research shows that despite the same method of measurement, the results of  $X_t/FrD$  at jet angle  $45^\circ$  have a difference of 97%.

### 3.2. Mathematical modeling results

The result of the mathematical model was captured after 17 seconds since the brine exit from jet nozzle. The time of data capturing was determined according to the observations made in the physical model.

Figure 8 shows a typical instantaneous image of the Mathematical modeling. Considering the range of Froude number in the physical experiments, the brine jet is simulated at four Froude numbers 7.3, 8.3, 12.6 and 15.6. The average of dimensionless numbers ( $X_t/FrD$  and  $Z_{max}/FrD$ ) is presented in the Table 2. CORJET, UM3, VISJET and JetLag are considered to be the most used commercial softwares for brine discharge modeling (Palomar et al., 2012).

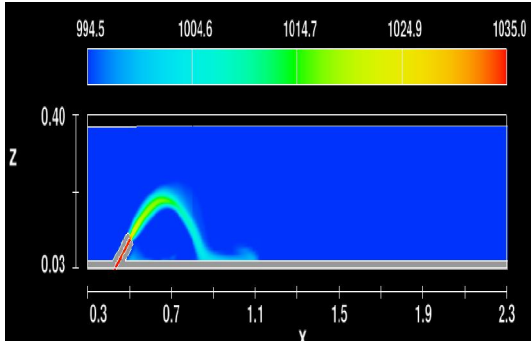


Figure 8 A typical instantaneous image of the Flow-3D (jet angle  $\Theta=45^\circ$ ,  $Q=0.22$  m<sup>3</sup>/hr,  $\rho_a=996$  kg/m<sup>3</sup> and  $\rho_j=1035$  kg/m<sup>3</sup>).

To have better comparison between the results of the Flow-3D and the other software, the results of these softwares and their Froude number range are also listed in Table 2.

Considering results presented in Table 2, the  $X_t/\text{Fr}D$  at jet angle  $60^\circ$  have been simulated by Flow-3D is compatible with the result of the current experiments and Kikkert et al. 2007.

The simulation result about  $X_t/\text{Fr}D$  at jet angle  $45^\circ$  is in a good agreement with results of

Kikkert et al. 2007, Cipolina et al., 2005, and Shao et al. 2010, But the result of flow-3D is about 25% less than the results of current experiments.

The result of Flow-3D about dimensionless number  $Z_{\text{max}}/D$  at jet angle  $60^\circ$  is relatively consistent with the results of Bloomfield et al., 2002 and UM3 Model (Palomar et al., 2012). But the result of flow-3D is about 45% less than the results of current experiments. Apparently, Numerical simulation of other models about  $Z_{\text{max}}/D$  at jet angle  $60^\circ$  is less than the experiments result conducted by another researchers (except the result of Bloomfield et al., 2002).

Finally, the result of Flow-3D about dimensionless number  $Z_{\text{max}}/D$  at jet angle  $45^\circ$  is 1.48. The value is in a good agreement with the result of CORJET. Also, it is in a very good agreement with Shao et al., 2010 and other researcher experiments (except the result of Nemlioglu and Roberts, 2006). The results of the mathematical models for the  $Z_{\text{max}}/D$  at jet degree  $45^\circ$  is very close to each other and the value is too close the experiments result (except the result of current study).

Table 2. Summary of experimental and mathematical modeling results about the maximum rise height and the horizontal location at  $Z_{\text{max}}$

| study                                | Method                   | Fr       | $Z_t/\text{Fr} D^*$ |      | $X_t/\text{Fr} D^*$ |      |
|--------------------------------------|--------------------------|----------|---------------------|------|---------------------|------|
|                                      |                          |          | 45                  | 60   | 45                  | 60   |
| Zeitoun et al. ,1970                 | Visual, fluorometry      | 25–60    | 1.56                | 2.13 | -                   | -    |
| Roberts and Toms, 1987               | Visual, fluorometry      | 12–26    | -                   | 2.08 | -                   | -    |
| Roberts et al. , 1997                | LIF, micro-conductivity  | 19–36    | -                   | 2.2  | -                   | -    |
| Bloomfield et al., 2002              | Visual                   | <20      | 1.24                | 1.63 | -                   | -    |
| Cipollina et al. , 2004              | Visual                   | 16-216   | 1.61                | 2.32 | 1.8                 | 1.42 |
| Nemlioglu and Roberts, 2006          | LIF                      | 22       | 2                   | -    | -                   | -    |
| Kikkert et al. ,2007                 | LA (laser attenuation)   | 14–99    | 1.6                 | 2.27 | 1.84                | 1.6  |
| Papakostantis and Christodoulou,2008 | -                        | -        | 1.59                | 2.16 | -                   | -    |
| Shao et al., 2010                    | PIV-LIF                  | 8–32     | 1.47                | -    | 1.69                | -    |
| Papakostantis et al., 2011           | Digital picture analysis | 7.5–58.3 | 1.58                | 2.14 | 2.1                 | 1.84 |
| Lai and Lee,2012                     | PIV-LIF                  | 10–40    | 1.58                | 2.08 | 3.34                | 2.84 |
| current study                        | Visual                   | 5.3-15.6 | 2.28                | 2.87 | 2.47                | 1.56 |
| Flow 3D, current study               | Mathematical Modeling    | 7.3–15.6 | 1.48                | 1.58 | 1.85                | 1.62 |
| CORJET, Palomar et al., 2012         | Mathematical Modeling    | 10–40    | 1.41                | 1.85 | 1.52                | 1.2  |
| UM3, Palomar et al., 2012            | Mathematical Modeling    | 10–40    | 1.24                | 1.60 | 1.32                | 1.09 |
| JetLag, Palomar et al., 2012         | Mathematical Modeling    | 10–40    | 1.27                | 1.69 | 1.52                | 1.32 |
| VISJET, Lai and Lee, 2012            | Mathematical Modeling    | 10–40    | 1.33                | 1.78 | 2.78                | 2.4  |

\*The values are equal to the average of all of experiments performed in the research.

#### 4. Discussions

Several studies conducted during the past five decades about the properties of inclined brine jet's trajectory. But unfortunately, the various results of these studies has caused confusion arise in this field. Using different methods to capturing the trajectory properties and choose different range of Froude number in various studies are two main reasons for this problem.

Comparing the experiments results of Lai and Lee, 2012, with the result of Shao et al. 2010, can be revealed that the range of Froude number on trajectory properties is highly effective. Despite having the same method, the average of dimensionless number  $X_t/\text{Fr}D$  of jet angle  $45^\circ$  Reported by Lai and Lee, 2010, is about two times of Shao et al. 2010 result.

In this study, the maximum rise of jet trajectory at angle  $45^\circ$  and  $60^\circ$  and relative horizontal

distance is investigated by experiments and a mathematical model (Flow-3D). The results show that the dimensionless numbers,  $X_t/FrD$  and  $Z_{max}/FrD$ , of round buoyant negative jet inclined  $45^\circ$  and  $60^\circ$  towards the horizon increases at small froude number ranged (range 5.3-15.6 at current study).

The results of mathematical model are shown that the Flow-3D has a good Capability to simulate the maximum rise and the horizontal distance of it. These results are in a good agreement with the results of Shao et al., 2010, Bloomfield et al., 2002 and Cipollina et al., 2004. Flow-3D simulates the value of dimensionless number  $X_t/FrD$  at angles  $45^\circ$  and  $60^\circ$  respectively, 25% and 1% lower than the experimental results. Also, the result of dimensionless number  $Z_{max}/FrD$  simulation is at angles  $45^\circ$  and  $60^\circ$  respectively, 35% and 45% lower than the experimental results.

#### Acknowledgements:

We would like to thank Ms. Masoud Dabir Vaziri, Faculty member of Islamic Azad University-South Tehran technical Branch, for his valuable help.

#### Corresponding author

Ph.D. candidate, Fariborz Mohammadi  
Department of Irrigation and Drainage, Water Science faculty, Chamran university of Ahwaz, Ahwaz, Iran.  
Cell Phone: +98-912-590-0833  
E-mail: [Mo.fariborz@gmail.com](mailto:Mo.fariborz@gmail.com)

#### 5. References

- Anwar, H.O., 1969. Behavior of buoyant jet in calm fluid. Journal of the Hydraulic Division, ASCE 95, 1289-1303. HY4, Proc. paper 6688.
- Bleninger, T. 1997. "Coupled 3D hydrodynamic models for submarine outfalls: Environmental hydraulic design and control of multiport diffuser", University of Karlsruhe, Institute for Hydromechanics.
- Bloomfield, L.J. and Kerr, R.C., 2002. Inclined turbulent fountains, Journal of Fluid Mechanics, vol. 451, Cambridge University Press, pp. 283-294.
- Cipollina, A., Brucato, A., Grisafi, F., Nicosia, S., 2005. Bench-Scale investigation of inclined dense jets. Journal of Hydraulic Engineering, ASCE 131 (11), 1017-1022.
- Doneker, R. L., and Jirka, G. H., 1999. "Expert systems for mixing-zone analysis and design of pollutant discharges." J. Water Res. Plng. and Mgmt., ASCE, 117(6), 679-697.
- Doneker, R.L., "Systems Development for Environmental Impact Assessment of Concentrate Disposal- Development of Density Current Simulation Models, Rule Base, and Graphical User Interface", DWPR Report No. 132, US Bureau of Reclamation, Denver CO, Aug. 2000.
- Fernandez-Torquemada, Y., Sanchez-Lizaso, J., Gonza lez-Correa, J., 2005. Preliminary results of the monitoring of the brine discharge produced by the SWRO desalination plant of Alicante (SE Spain). Desalination 182, 395-402.
- Flow Science, 2003. FLOW-3D. [Theory manual]. Los Alamos, NM.
- Gacia, E., Invers, O., Manzanera, M., Ballesteros, E., Romero, J., 2007. Impact of the brine from a desalination plant on a shallow seagrass (*Posidonia oceanica*) meadow. Estuarine, Coastal and Shelf Science 72, 579-590.
- Iso, S., Suizu, S., Maejima, A., 1994. The lethal effect of hypertonic solutions and avoidance of marine organisms in relation to discharged brine from a desalination plant. Desalination 97, 389-399.
- Jirka, G. H., 2004. Integral model for turbulent buoyant jets in unbounded stratified flows. Part I: The single round jet. Environ. Fluid Mech., vol. 4, pp. 1-56.
- Jirka, G., 2008. Improved discharge configurations for brine effluents from desalination plants. Journal of Hydraulic Engineering 134, pp. 116-120.
- Kikkert, G.A., Davidson, M.J., Nokes, R.I., 2007. Inclined negatively buoyant discharges. Journal of Hydraulic Engineering, ASCE 133 (5), 545-554.
- Kim, D.G. and Cho, H. Y., 2006. Modeling the buoyant flow of heated water discharged from surface and submerged side outfalls in shallow and deep water with a cross flow. Environ Fluid Mech. 6, 501-518.
- Lai, C.C.K., Lee, J. H. W., 2012. Mixing of inclined dense jets in stationary ambient. Journal of Hydro environment Research. Vol. 6, 9-28.
- Nemlioglu, S. and Roberts, P.J.W. 2006. Experiments on dense jets using three-dimensional laser-induced fluorescence (3DLIF), Proc. MWWA 2006, 4th International Conference on Marine Waste Water Disposal and Marine Environment, Antalya, Nov. 6-10.
- Palomar, P. Lara, J.L. and Losada, I.J. 2012. Near field brine discharge modeling part 2: Validation of commercial tools. Desalination 290, 28-42.
- Papakostantis, I.G., Christodoulou, G.C., Papanicolaou, P.N., 2011a. Inclined negatively buoyant jets 2: concentration measurements. Journal of Hydraulic Research 49 (1), 13-22. n.d.
- Roberts, D.A., Johnston, E. L., Knott, N. A. "Impacts of desalination plant discharges on the marine environment: A critical review of published studies." (water research) 44 (2010): 5117-5128.
- Roberts, P.J.W., Ferrier, A., Daviero, G., 1997. Mixing in inclined dense jets. Journal of Hydraulic Engineering, ASCE 123 (8), 693-699. n.d.
- Sadhvani, J., Veza, J., Santana, C., 2005. Case studies on environmental impact of seawater desalination. Desalination 185, pp. 1-8.
- Shao, D., Law, A.W.K., 2010. Mixing and boundary interactions of 30 and 45 inclined dense jets. Environmental Fluid Mechanics 10. 521-553.
- Yakhot V, Orsarg SA, Thangam S, Gatski TB, Speziale CG (1992) Development of turbulence models for shear flows by a double expansion technique. Physics Fluids 4(7):1510-1520.
- Yakhot, V., Orszag, S.A. 1986 Renormalization group analysis of turbulence. I. Basic theory. J Scientific Computing 1(1):1-51.
- Zeitoun, M.A., Reid, R.O., McHilheny, W.F., Mitchell, T.M., 1970. Model Studies of Outfall System for Desalination Plants. Research and Development Progress Rep. 804. Office of Saline Water, U.S. Dept of Interior, Washington, D.C.

2/11/2012